2018 HAWAII UNIVERSITY INTERNATIONAL CONFERENCES
STEAM - SCIENCE, TECHNOLOGY & ENGINEERING, ARTS, MATHEMATICS & EDUCATION
JUNE 6 - 8, 2018 PRINCE WAIKIKI, HONOLULU, HAWAII

COMPARISON OF EXPERIMENTAL TWO-PHASE FLOW AND THEORETICAL POISEULLE-COUETTE FLOW AT LOW REYNOLDS NUMBERS

MADAD, REZA
MECHANICAL ENGINEERING DEPARTMENT
THE UNIVERSITY OF AKRON
AKRON, OHIO

Dr. Reza Madad
Mechanical Engineering Department
The University of Akron
Akron, Ohio

Comparison of Experimental Two-Phase Flow and Theoretical Poiseulle-Couette Flow at Low Reynolds Numbers

Synopsis:

The fully developed air-water flow is studied experimentally in a high aspect ratio air-water tunnel facility with Pitot-tube and laser Doppler velocimetry (LDV) measurements. The experimental techniques and consideration are explained in this article. The Poiseuille-Couette flow (PCF) with solid moving wall is simulated to facilitate the comparison of air-water flow with the smooth water surface and PCF with a solid wall.

COMPARISON OF EXPERIMENTAL TWO-PHASE FLOW AND THEORETICAL POISEUILLE-COUETTE FLOW AT LOW REYNOLDS NUMBERS

ABSTRACT

The fully developed air-water flow is studied experimentally in a high aspect ratio air-water tunnel facility with Pitot-tube and laser Doppler velocimetry (LDV) measurements. The experimental techniques and consideration are explained in this article. The airflow is studied in the Reynolds number range of $1000 < Re < 4500$ from laminar to turbulent regimes. The Poiseuille-Couette flow (PCF) with solid moving wall is simulated to facilitate the comparison of air-water flow with the smooth water surface and PCF with a solid wall. The results show the agreement of these two flows in first-order statistics. However, the higher–order statistics such as energy components for the water side doesn't agree because of the transferred energy of airflow to the large mass of still water. This study suggests using one-phase PCF simulation for low Reynolds numbers to acquire the first-order statistics since it is accurate and economical.

Keywords: *Two-phase, PCF, LDV, Air-water tunnel*

INTRODUCTION

The interaction between a moving liquid and gas flowing adjacent to the liquid has been a subject of many investigations due to its application in industries, geophysical and environmental sciences (Banerjee 2007). The environmental applications of two-phase flow interaction are the exchange of greenhouse gases between the atmosphere and the oceans, and the aeration of lakes and rivers.

Several experimental and numerical studies have been conducted to investigate the effects of the liquid-gas interaction on the air flow and liquid flow in a smooth or wavy liquid surface in the horizontal open and closed channels (e.g., (Fulgosi, et al. 2003), (Spencer, et al. 2009), and (Longo and Losada 2012)). Because of the difficulties in measuring the velocity fields in the vicinity of moving surfaces and the complexity of two-phase flow simulating, there is still a lack of understanding the gas motion near deforming interfaces.

The objective of this article is to study the experimental techniques to acquire the data with the minimum error and investigate the similarities and differences of two-phase flow and Poiseuille-Couette flow (PCF).

EXPERIMENTAL SET-UP

In this section, the important details of air-water tunnel facility construction are provided. The experiment is performed in a glass water tank with a total length of 12m, and inside depth and width of 600mm and 300mm, respectively. A return pump and water plumbing pipes are located beneath of the tank. The air-water tunnel is located in the middle of the tank, 3m away from the tank's ends. The air-water tunnel facility consists of an inlet, contraction, test section, diffuser, vaned corner, and a suction fan. A schematic of the air-water tunnel facility placed on the tank is shown in figure 1.

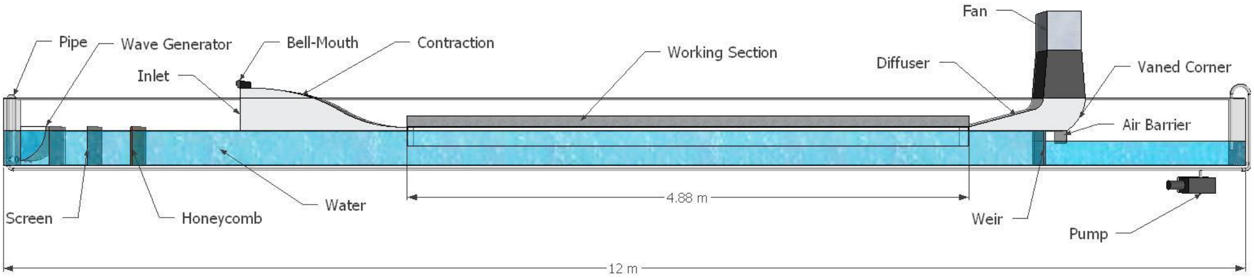

Figure 1 - Schematic of air-water tunnel facility

An 11:1 width-to-height ratio was chosen to nominally satisfy the requirement of two-dimensionality of the airflow. The facility is made mostly from acrylic and hung by ball screw rods in order to adjust its height and inclination. Longitudinal and lateral alignment was achieved using a digital level and string line. The longitudinal and lateral deflection of less than ±0.05 degrees is present along the entire tunnel. While the fan is running, the change in the water height generates different area ratio along the working section of the channel. In order to achieve a linear pressure distribution along the working section, a moveable ceiling is required. The inclination of the upper wall of the working section is adjusted to provide the same inclination as the water surface. The entrance part of the working section fixed to the contraction section and the exit part is adjusting using the ball screw rods (see figure 2).

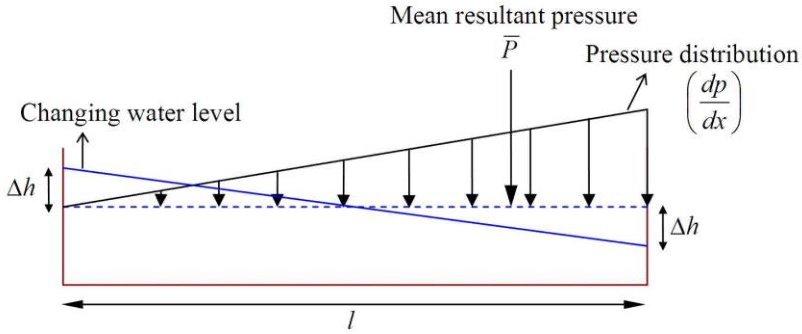

Figure 2 - Pressure distribution changes water level

While the water motion was generated by the air flow, one stagnation line appeared close to the diffuser and disrupted the water motion, generating an instability in the air flow. Several techniques were tried to solve this problem. Eventually, a weir in combination with a very slight water pumping was chosen. The weir prevented any effect of the downstream flow on the upstream flow. Also, to prevent any effect of foreign matter on the experiment, an air barrier was used at the end of the tunnel.

MEASUREMENT TECHNIQUES

The measuring section was set up 3.5m from the inlet and 3.4m from the exit. This location was chosen with the expectation that the flow would be fully developed; i.e., the development length is more than *170H*, where *H* is tunnel height. To confirm the fully developed flow, fifteen static pressure taps were inserted in the tunnel upper wall. Figure 3 shows the pressure coefficient (C_P) plotted against streamwise position normalized by total tunnel's working section length (*x/L*) at friction Reynolds number of $\delta^+ = 135$. The last six pressure taps form a nearly linear trend, indicating nominally fully developed flow.

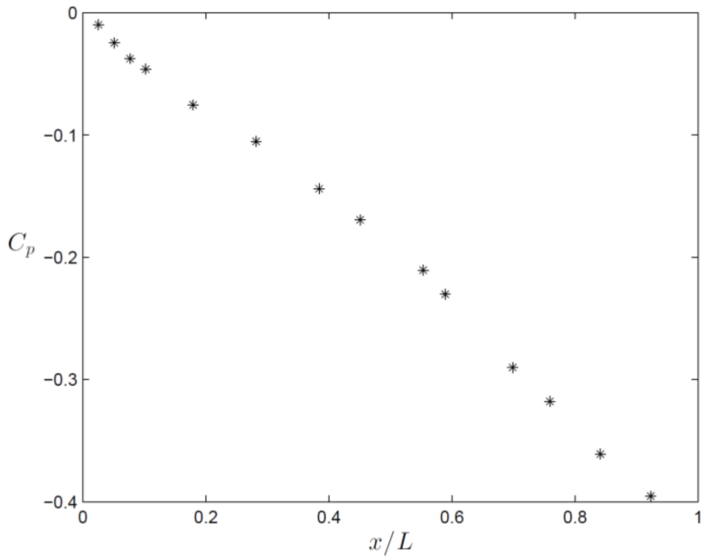

Figure 3 - Pressure gradient versus streamwise distance normalized by working length

A Pitot-static tube was used to measure streamwise mean velocity profiles at *x = 173H* downstream of the channel inlet. The total pressure is measured with the Pitot-tube and the static pressure is determined with pressure taps close to the measurement station. The Pitot-tube used in the channel flow is shown in figure 4.

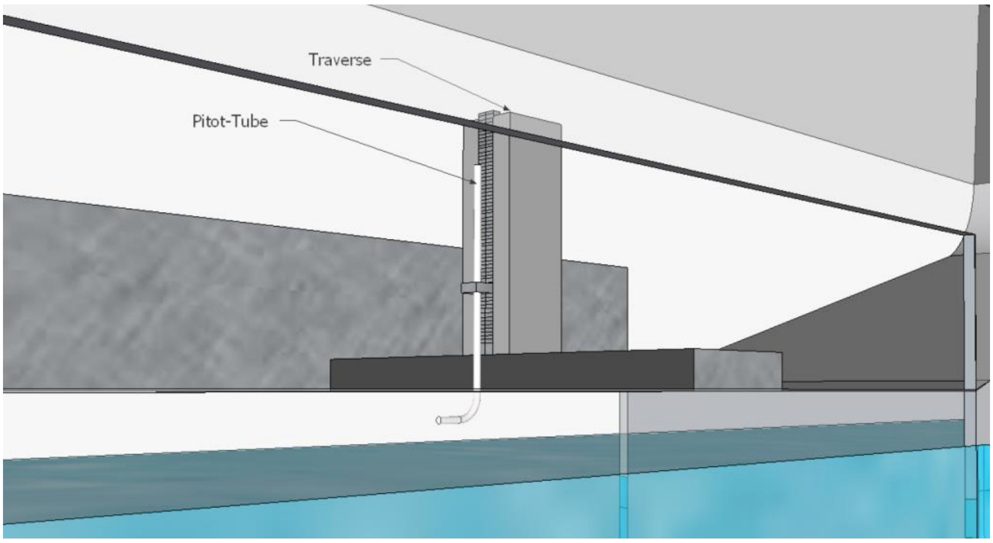

Figure 4 - Schematic of Pitot-tube used in experiment

The velocity measurement techniques such as impact tubes, hot-wire, and hot-film anemometry introduce difficulties due to probe interference with the flow and problems arising from the presence of liquid vapor inside the gas phase. Particle image velocimetry (PIV) as another technique is also difficult to measure the liquid velocity in gas-liquid flow because the voids interfere with the light sheet illumination and it is difficult to separate the continuous and dispersed phases. In the current experiment, the laser Doppler velocimetry (LDV) is used to measure the velocity without interfering the flow. The LDV system is calibrated with three procedures of spinning disk (Park, Cutbirth and Brewer 2002), spinning wire (Kurihara, Terao and Takamoto. 2002), and Pitot-tube measurements. The spinning disk calibration is shown in figure 5.

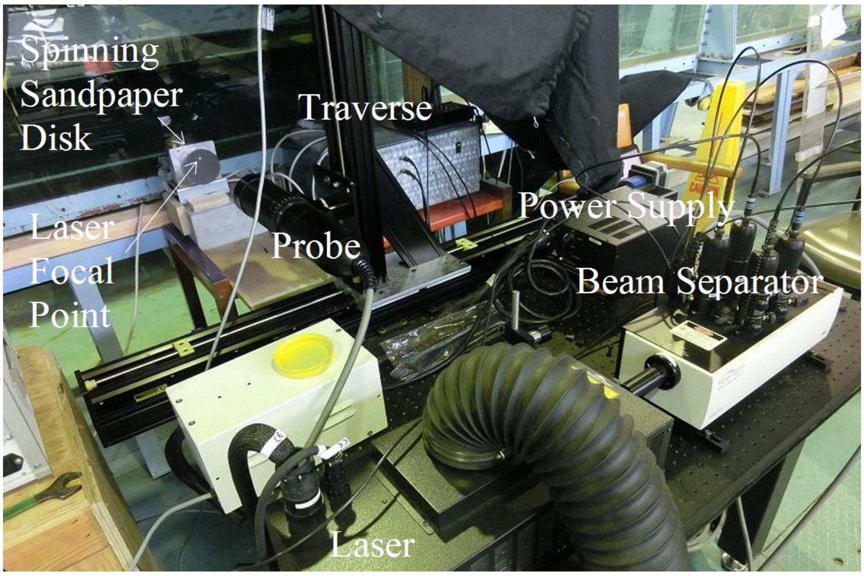

Figure 5 - LDV calibration with spinning disk

Obtaining LDV measurements close to the air-water interface is challenging. Two different methods were employed to address this challenge. First, by rotating the LDV probe and aiming the lasers at the water surface from top and underneath of the interface, the water surface velocity was measured. Second, one video camera was mounted on top of the channel facing down the test section while the water surface was seeded with insoluble Polyethylene fluffs of specific gravity of 0.95. A floatable ruler was used to measure the actual distance between captured particles moving with the water surface. The average velocities obtained from these two methods were quite similar, with less than 5% difference.

RESULTS

The inner normalized mean velocity profiles over the friction Reynolds number range of $40 \leq \delta^+ \leq 144$ is presented in figure 6. The lowest Reynolds number is in the laminar regime and the highest is for flow with small ripples on the water surface. In figure 6, the water surface is at $y = 0$. The Reynolds numbers, friction Reynolds numbers of stationary wall and corresponding symbols are shown in table 1.

Table 1 - Reynolds numbers and symbols

Re	$\delta^+{}_{sw}$	Symbol
1170	40.4	×
2237	76.0	▽
2271	77.4	∗
2581	86.9	+
2958	101.1	◇
3683	118.2	◁
1170	124.5	□
3836	130.9	○
4003	135.3	△
4267	143.7	☆

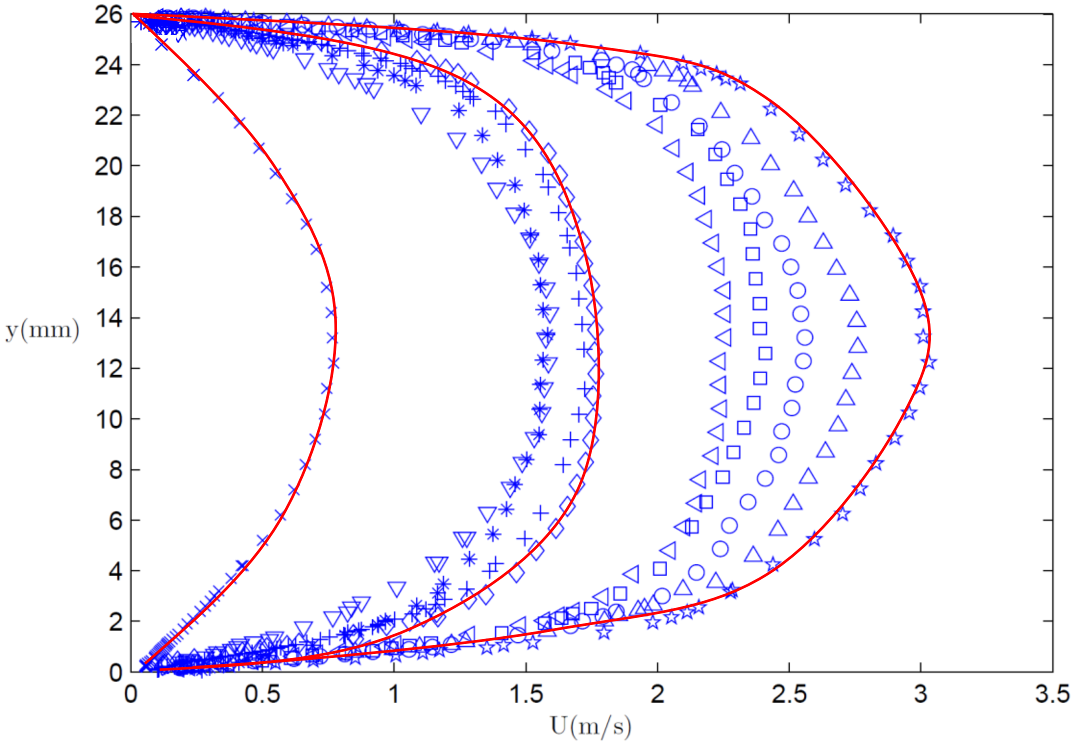

Figure 6 - Mean velocity profiles at different Reynolds numbers

The Poiseuille-Couette Flow (PCF) with a solid moving wall is simulated with a direct numerical simulation (DNS) method to compare with the current results at the same Reynolds numbers. The mean velocity profiles of only three Reynolds numbers obtained from DNS are shown in figure 6 with solid red lines. The experimental data are in a very good agreement with the simulation.

The velocity profile of the turbulent airflow at the friction Reynolds number of $\delta^+ = 135$ and interacted water flow obtained from LDV measurements are shown in figure 7. The layers of the water in the tank is moved relatively slow on top of each other by interacting with the airflow.

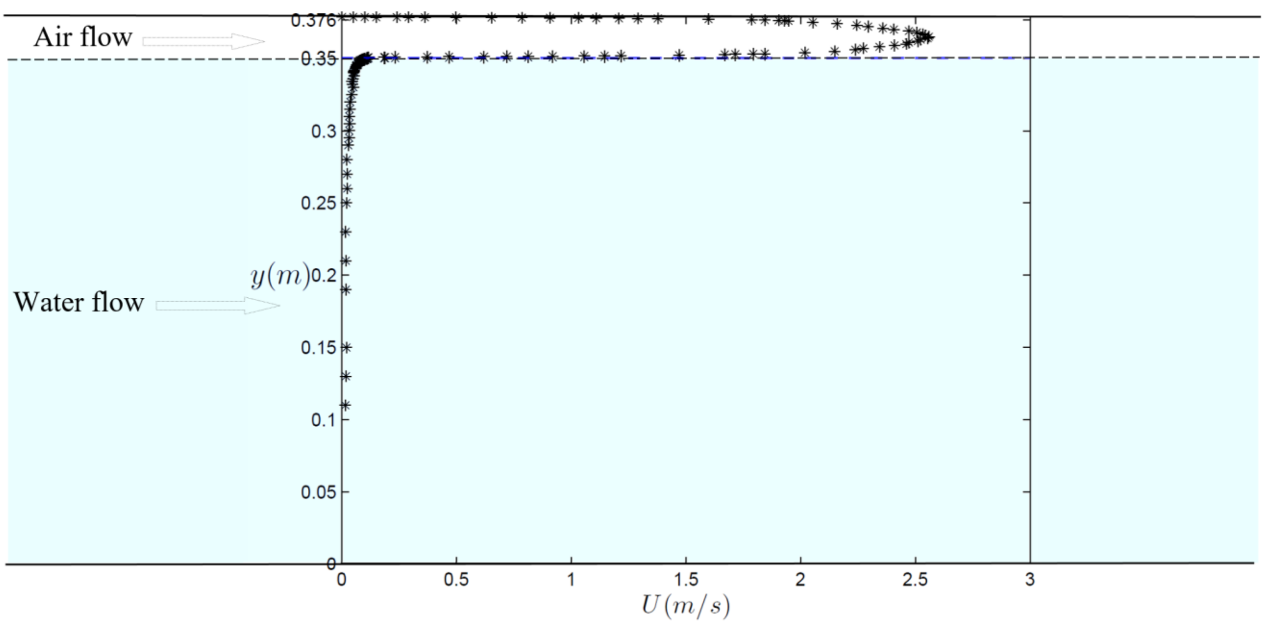

Figure 7 - Velocity profile of turbulent airflow on top of the water flow from experimental data at $\delta^+ = 135$

The turbulent kinetic energy production profiles normalized by the stationary wall friction velocity, $E_p^+(y) = -<uv>^+ (\delta U^+/\delta y^+)$, for the experiment and simulation are shown in figure 8. Both profiles exhibit consistent results with diminishing energy production close to the channel centreline and peaks near both walls with amplification of E_p^+ near the stationary wall and attenuation near the moving wall. The peak near the moving wall (DNS) is higher than the peak near the moving water surface (experiment). The net energy production (area under profile) for simulated PCF is 5% larger than experiment.

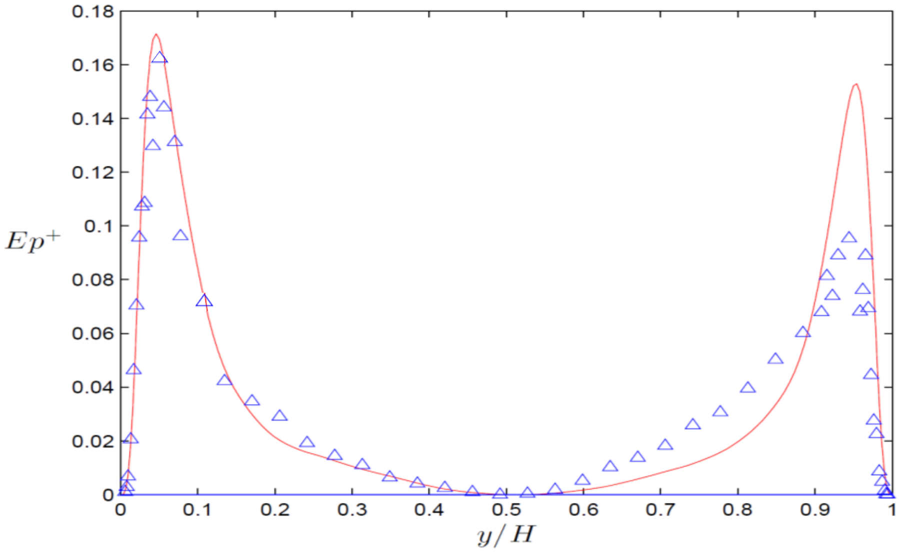

Figure 8 - Normalized turbulent kinetic energy production profiles of the experiment and simulation

The streamwise premultiplied energy spectra of results of the current experiment and simulated data of the Poiseuille-Couette flow at the same wall-normal position are shown in figure 9. These spectra reveal that the DNS data shows larger energy spectra peak than flow with moving water, especially close to the moving wall (figure 9(b)).

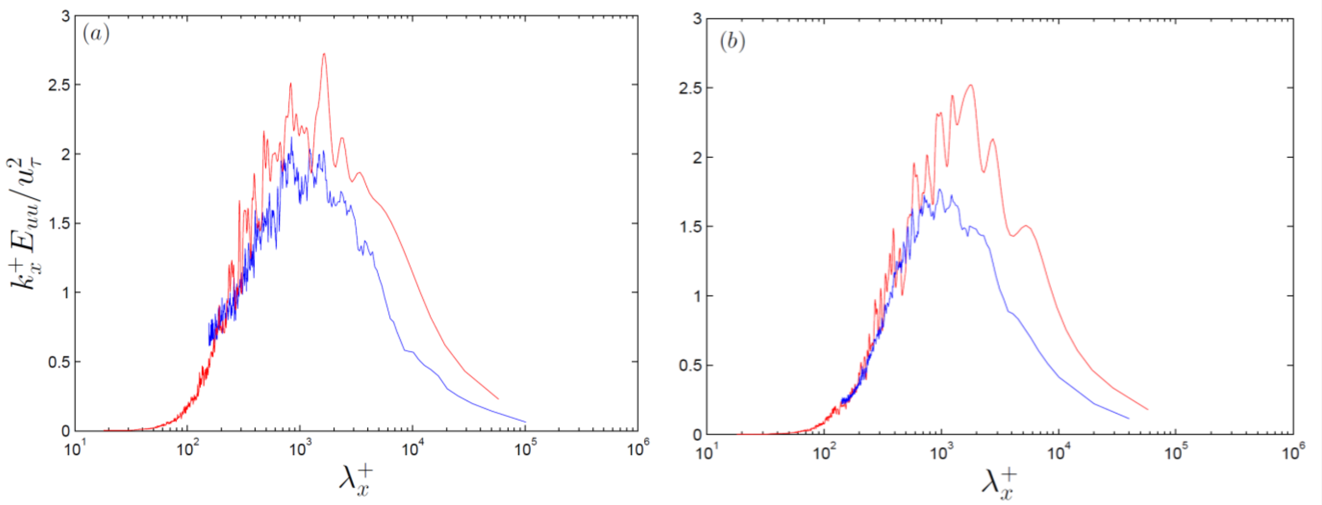

Figure 9 - Streamwise premultiplied energy spectra close to the stationary wall (a) and moving wall (b). Red line represents the DNS results and blue line shows the experimental data

CONCLUSION

After considering the accurate experimental techniques, the air-water flow experiment at low Reynolds numbers range without with smooth air-water interface is conducted. The Poiseuille-Couette flow with a solid moving wall is simulated to compare with current experiment. The comparison shows the agreement in mean velocities of airflows and discrepancies in second-order statistics. In particular, the energy of the airflow at PCF shows larger value than two-phase flow. The energy of the airflow is transmitted to the water and consumed to overcome the drag of the large mass of water tank and the amount of the energy transported to the water is higher than the energy transported to the solid moving wall. It could be concluded that more airflow energy is consumed in maintaining the movement of the almost still water compared to the airflow with moving solid wall.

This study suggests the PCF simulation for low Reynolds numbers with smooth water surface rather than experiment for acquiring first-order statistics such as mean velocities, since the two-phase experiment is costly and time-consuming. However, for higher-order statistics of airflow the PCF simulation for the water side of the air-water tunnel is not reliable and two-phase DNS is recommended.

References

Banerjee, S. 2007. *Transport at the Air-Sea Interface.* Springer Berlin Heidelberg,.

Fulgosi, M, D Lakehal, S Banerjee, and V D Angelis. 2003. "Direct numerical simulation of turbulence in a sheared air water flow with a deformable interface." *Journal of Fluid Mechanics* 319:482.

Kurihara, N, Y Terao, and M Takamoto. 2002. "LDV calibration for the air speed standard between 1.3 to 40 m/s." *International Symposium on Fluid Flow Measurement.* Virginia. 61.

Longo, S, and M A Losada. 2012. "Turbulent structure of air flow over wind-induced gravity waves." *Exp. Fluids* 369:390.

Park, J T, J M Cutbirth, and W H Brewer. 2002. *Hydrodynamic performance of the Large Cavitation Channel.* California: Technical Report NSWCCD-5-TR.

Spencer, N B, L L Lee, R N Parthasarathy, and D V Papavassiliou. 2009. "Turbulence structure for plane Poiseuille Couette flow and implications for drag reduction over surfaces with slip." *Can. J. Chem.* 38:87.